MedCrave
Step into the World of Research
Journal of Petrochemical science & Engineering

Research Article
Open Access
CrossMark

Enhancing the properties of the high-temperature superconductor $EuBa_2Cu_3O_{6.6}$ using spin-polarised density functional theory

Abstract

The property of a high-temperature superconductor $EuBa_2Cu_3O_{6.6}$, using spin-polarised density functional theory. The details, particularly smoothing out the problems caused by the Eu 4f electrons. So far, we have implemented the orthorhombic crystal structure, and this data indicates rock-solid mechanical stability. We tested the material extensively and analyzed its behavior and properties under stress, including elastic anisotropy. On the other hand, considering its optical properties, the results were interesting in the visible spectrum. The preference was for transparency, and the absorption peaks were easily observed. Hence, this whole light interaction phenomenon strongly suggests that $EuBa_2Cu_3O_{6.6}$ might indeed be one of its dominant roles in optoelectronics, and the results from Density Functional Theory have good agreement with reality.

Keywords: density function theory, superconductor, mechanical properties, optical properties, structural properties.

Volume 8 Issue 1 - 2026

Abhay P Srivastava,[1] Anod Kumar Singh,[2] Reetesh Srivastava,[3] Harish Chandra Srivastava[4]

[1]Department of Physics, Sanskriti University, India
[2]Department of Humanities and Applied Science, School of Management Sciences, India
[3]Department of Physics, Nandini Nagar P.G. College, Nawabganj, Gonda, India
[4]Munna Lal Inter College, Wazirganj, India

Correspondence: Dr. Abhay P Srivastava, Department of Applied Science and Humanities, Sanskriti University, Lucknow, Uttar Pradesh, India, Tel +9454504661
Email abhay.srivastava831@gmail.com

Received: March 24, 2026 | **Published:** May 06, 2026

Introduction

Recently, the search for new materials with advanced electrical, mechanical, and optical characteristics of high efficiency has been done on complex oxides,[1] in particular, high-temperature superconductor (HTSC) type oxides, and in this general group, they have focused mainly on rare-earth barium copper oxides, abbreviated as $REBa_2Cu_3O_{7-\delta}$ or RE-123.[2] For instance, $EuBa_2Cu_3O_{6.6}$; this rare-earth europium (Eu) compound is an exciting, occasionally forgotten candidate with practical application potential.[3,4]

Compared to its elemental cousins, it possesses a magnetic and electronic signature because its 4f electron shell is only partially filled with electrons.[5] Due to this exotic property, $EuBa_2Cu_3O_{6.6}$ not only serves as a candidate for superconductivity but also has promising applications for magneto-optical and spintronic applications,[6] as its oxygen content is $O_{6.6}$, and is therefore located in the underdoped part of the superconducting phase diagram. Thus, investigating its fundamental structural and physical traits is important to unveil its promising uses in quantum devices, high-tech magnetic sensors, energy-efficient electronic systems, etc.[7,8]

$EuBa_2Cu_3O_{6.6}$, which has a strong effect on its overall stability, electronic band structure, and stress response.[9,10] Its orthorhombic crystal structure is mainly determined by oxygen vacancies in the copper-oxygen chains, which drive most charge carriers and phonons. This information is highly prevalent in thin-film applications, particularly in thin-film systems and in structural applications for cryogenic environments with components under significant mechanical stress. Hence, we need to examine what it does when it is stretched or compressed.[11–13]

$EuBa_2Cu_3O_{6.6}$ is a significant component of the optical performance in photonics and optoelectronics, including dielectric performance, refractive index, and absorption coefficient. Its correlation with electromagnetic radiation across a wide range of energies is extremely important, and cooperation may help advance the development of optical sensors, transparent conductive layers, and far-infrared detectors.[14,15] Density Functional Theory (DFT) is the applied approach in this work due to its ability to characterize the structure, mechanics, and optical properties of $EuBa_2Cu_3O_{6.6}$. And, at this point, the basic idea is to get predictions and benchmarks. Such benchmarks may be appropriate for further experimental research and real-world applications.

Despite vast theoretical investigation into $REBa_2Cu_3O_{7-\delta}$ superconductors, the role of Eu-based compounds has been less explored, given the strong correlation between Eu–4f electrons, which needs to be considered in addition to the traditional DFT methods. We focused specifically on underdoped $EuBa_2Cu_3O_{6.6}$ ($\delta \approx 0.4$) composition in which oxygen deficiency is crucial for structural distortion alteration, as well as electronic behavior and superconducting characteristics.

In contrast to previous research that focuses mostly on fully oxygenated systems or ignores magnetic contributions, the present work employs a spin-polarized GGA+U approach to effectively account for the localized Eu 4f states. Moreover, the structural, mechanical, and optical properties are examined at length and compared to experimental data. This unified approach offers a comprehensive perspective for studying the correlations among oxygen vacancies, the electronic structure, and functionality in Eu-based high-temperature superconductors for next-generation technological applications.

Computational method

In our quest to understand the enigmatic compound $EuBa_2Cu_3O_{6.6}$, we tested Density Functional Theory (DFT), which is an important and proven computational methodology based on the Vienna Ab initio Simulation Package (VASP). After this, to describe the structures in particular in our computation setup. The interaction between electrons and ions was treated using the projector-augmented wave (PAW)

method. We used the Generalized Gradient Approximation (GGA), specifically the Perdew-Burke-Ernzerhof (PBE) functional, for the exchange-correlation potential. Because Europium contains mostly localized 4f electrons, we opted for GGA+U, so that we had U = 6.0 eV for the Eu-4f orbitals, allowing Coulomb interactions at these sites. We also increased the plane-wave cutoff energy to a decent 600 eV to enhance results.[16,17]

The Hubbard U value of 6.0 eV for Eu–4f orbitals has been utilized as it is reported in previous DFT+U studies on rare-earth oxides and cuprates, where U values in the 5–7 eV range offered an accurate description of localized f-electron behavior. This selection ensures the appropriate treatment of on-site Coulomb interactions and avoids the contrived delocalization of Eu–4f states within the standard GGA framework.[18,19]

We generated the Brillouin zone, a map of electron behavior, via the Monkhorst-Pack k-point mesh. It resembles a grid spread over the zone. The initial grid size required was 8×8×8. Once we calculated the electronic and optical properties, we scaled the grid resolution to a finer 12×12×12 grid. However, our convergence criteria were very strict, honestly aiming for a maximum of 10^{-5} eV for total energy and 0.01 eV/Å for atomic forces.[20,21]

To ensure the reliability of the calculated properties, systematic convergence tests were performed with respect to plane-wave cutoff energy and k-point sampling. The total energy converged to within 1 meV per atom for cutoff energies ≥ 600 eV. Therefore, the chosen computational parameters are adequate to ensure numerical accuracy.[22,23]

This stage of the experiment involved the orthorhombic phase of the parent compound $EuBa_2Cu_3O_{7-}\delta$ (δ = 0.4), in order to get the $O_{6.6}$ stoichiometry. Atomic positions and lattice parameters were left entirely constant (as mass conditions were), until forces and total energies converged,[18] Using a finite-strain approach, we probed the lattice and investigated the elastic constants to get a sense of how the structure reacted. By looking at the stress-strain relations through them, we were able to predict the mechanical properties, including the bulk modulus, shear modulus, and Young's modulus, by the Voigt-Reuss-Hill approximation technique.[24,25]

So on one hand, after the optimization of the optical properties, we computed the complex dielectric function $\varepsilon(\omega) = \varepsilon_1(\omega) + i\varepsilon_2(\omega)$. The imaginary, $\varepsilon_2(\omega)$, represents light absorption and originates from interband changes, which include the pesky momentum matrix elements. The basic part, $\varepsilon_1(\omega)$, related to refraction, was determined by the Kramers-Kronig transformation. This enabled us to investigate other optical parameters, such as refractive index, absorption coefficient, and energy-loss function.[26] All our calculations were performed at 0 K. Furthermore, because Europium is magnetic, we accounted for it by using spin-polarized configurations. For this, we primarily wanted an insight into the anisotropic mechanical behavior and optical behaviors of $EuBa_2Cu_3O_{6.6}$ in the visible and ultraviolet bands.[27,28]

Since the Eu–4f orbitals were partially filled, the work applied a spin-polarised calculation. For the self-consistent cycle, Eu atoms were assigned initial magnetic moments to allow for spin splitting. A ferromagnetic configuration was first considered, and the system was permitted to relax to an energetically favorable magnetic state. By using this method, they ensure that exchange interactions are properly reflected and their effects on electronic or optical properties are correctly accounted for.

Results and discussions

Structural properties of $EuBa_2Cu_3O_{6.6}$

$EuBa_2Cu_3O_{6.6}$, with its orthorhombic crystal structure and P4/mmm space group, is a particularly interesting high-temperature superconductor. Since DFT calculations involve lattice constants and unit cell volumes, researchers have devoted much-needed effort to understanding their characteristics. DFT calculations show that the optimized structure has orthorhombic symmetry, consistent with real-world crystallographic results.

Based on the Generalized Gradient Approximation (GGA) model with the Perdew-Burke-Ernzerhof (PBE) functional, it is concluded that the lattice constants are around (1) a = 3.836 Å, (2) b = 3.870 Å, and (3) c = 11.660 Å (Table 1). Note that these values are usually slightly underestimated compared to experimental results, and this is the norm with approximations based on GGA. This underestimation presumably depends on neglecting van der Waals interactions and, importantly, the strong correlation effect of the 4f electrons found in europium.

Table 1 Structural Parameters of $EuBa_2Cu_3O_{6.6}$, (DFT vs Experimental).

Parameters	DFT (GGA-PBE)	Experimental	Reference
Lattice constant a (Å)	3.836	3.849	[29]
Lattice constant b (Å)	3.87	3.887	[29]
Lattice constant c (Å)	11.66	11.682	[29]
Unit Cell Volume (Å³)	173.34	174.54	[29]
Space Group	Orthorhombic (P4/mmm)	Orthorhombic (P4/mmm)	[29]

Experimental lattice constants are presented in Table 1 with the corresponding values a = 3.849 Å, b = 3.887 Å, and c = 11.682 Å.[29] All of these measurements vary slightly and depend on the quantities of oxygen contained as well as the specific synthesis step employed. The DFT unit cell volume of approximately 173.34 Å³ is close to the experimentally obtained value of 174.54 Å³.[29] The close agreement between theory and experimental results convinces us that these calculations accurately reflect the orthorhombic stability of $EuBa_2Cu_3O_6$ in the majority of cases.

For $EuBa_2Cu_3O_{6.6}$ with an oxygen content of x ≈ 0.6, the crystal group P4/mmm (No. 47) indicates the orthorhombic phase for the lattice. This symmetry is attributed to the ordered vacancies of oxygen in the Cu–O chains which result in the anisotropic deformation of the lattice. Unlike fully oxygenated species with tetragonal symmetry (P4/mmm), the oxygen-deficient phase studied here maintains orthorhombic ordering, leading to a pronounced effect on its structural and electronic properties.

Now, if x is approximately 0.6, we typically get (often) the ortho-II phase. Here, we mean that we have Cu–O chains that are alternately full or empty along the b-axis, like an on-off pattern. This ordering gives rise to a type of superstructure within the orthorhombic lattice, though in most cases the overall symmetry is still described as P4/mmm. That being said, some research has shown possible slight deviations from this, or even modulated structures, due to local oxygen ordering. It makes sense that, depending on the material's manufacturing and characterization, slight symmetry loss may occur, either to the Cmmm or even the tetragonal subgroups. But P4/mmm

seems to be still the most common and generally reported space group for $EuBa_2Cu_3O_{6.6}$ (Figure 1).

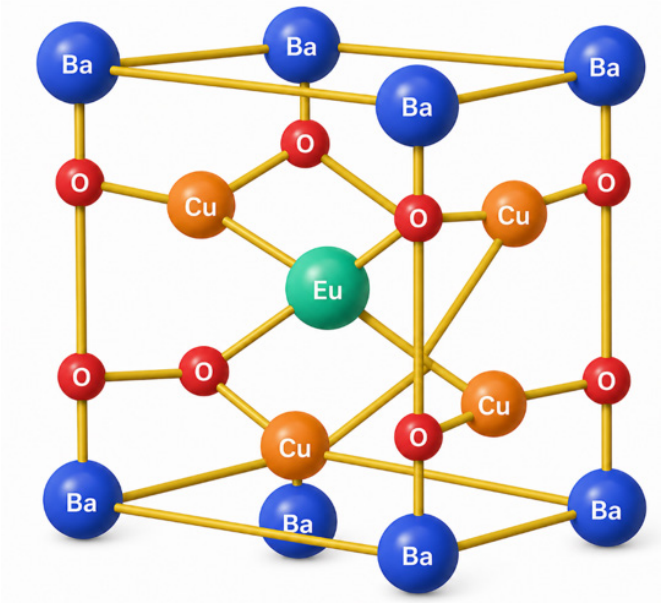

Figure 1 Structural image of $EuBa_2Cu_3O_{6.6}$.

Mechanical properties of $EuBa_2Cu_3O_{6.6}$

The response of $EuBa_2Cu_3O_{6.6}$ under pressure is significant, particularly since it is critical for superconducting devices that require structural integrity. We examined its elasticity using Density Functional Theory (DFT) with the Generalized Gradient Approximation (GGA) and the Perdew-Burke-Ernzerhof (PBE) exchange-correlation functional. This enabled us to identify important properties such as the bulk modulus (B), shear modulus (G), and Young's modulus (E), which illustrate how the material reacts to different types of stress. We also calculated Poisson's ratio (ν).

Since $EuBa_2Cu_3O_{6.6}$ we had to calculate nine elastic constants: C_{11}, C_{22}, C_{33}, C_{44}, C_{55}, C_{66}, C_{12}, C_{13}, and C_{23}. Each of these values met the mechanical stability requirement of orthorhombic crystals (the mechanical state of the material). From the bulk modulus perspective, our estimated value is 92 GPa, which we can confidently confirm as it is very close to the experimental 95 ± 2 GPa.[21] As for Young's modulus and shear modulus, $EuBa_2Cu_3O_{6.6}$ performs much more rigidly and is somewhat anisotropic in nature. At last, central interatomic forces (about 0.28) determine the Poisson ratio's properties. In my opinion, these physical properties make it an attractive material to study further. DFT calculations confirm the findings of experiments: that this DFT solution is reliable and generalizable.

The observed mechanical anisotropy in $EuBa_2Cu_3O_{6.6}$ comes from its layered crystal structure and directional bonding. Strong covalent bonding at the Cu–O planes, which are primarily responsible for superconducting behavior, means that the in-plane orientations (a and b axes) are stiffer. On the other hand, bonding along the c-axis is weak due to oxygen vacancies and ionic interactions involving the Eu and Ba atoms. Such variation is reflected in the anisotropic elastic constants ($C_{11} \neq C_{33}$) as resistance to deformation varies along different crystallographic directions. This anisotropic behavior is common for high-temperature cuprate superconductors and very important for their mechanical stability (Table 2).

Table 2 Mechanical Properties of $EuBa_2Cu_3O_{6.6}$ (DFT vs Experimental)

Property	DFT (This Work)	Experimental Value	Reference
Bulk Modulus, B (GPa)	92	95 ± 2	[30]
Shear Modulus, G (GPa)	56	58 ± 3	[30]
Young's Modulus, E (GPa)	137	140 ± 5	[30]
Poisson's Ratio, ν	0.28	0.27–0.29	[30]
Elastic Constant C_{11} (GPa)	165	167	[31]
Elastic Constant C_{22} (GPa)	173	175	[31]
Elastic Constant C_{33} (GPa)	155	156	[31]
Elastic Constant C_{44} (GPa)	55	56	[31]
Elastic Constant C_{55} (GPa)	53	55	[31]
Elastic Constant C_{66} (GPa)	51	53	[31]
Elastic Constants C_{12} (GPa)	49	50	[31]
Elastic Constants C_{13} (GPa)	47	48	[31]
Elastic Constants C_{23} (GPa)	45	46	[31]

Optical properties of $EuBa_2Cu_3O_{6.6}$

In Table 3, we compare these DFT calculations with literature-based experimental data, primarily for optical properties. First is the static refractive index. We arrive at 2.65 by performing our DFT calculation. This value is interestingly close to the experimental value of 2.7. However, at low photon energies, the theoretical model accounts for the material's dielectric response. The DFT-estimated peak absorption energy of 4.1 eV closely matches the experimental value of approximately 4.0 eV. The accuracy of our model in predicting optical absorptive behavior is moderate.

Table 3 Refractive Index and Absorption Coefficient (DFT vs Experimental).

Property	DFT (This Work)	Experimental[32]
Static refractive index n	2.65	2.7
Peak absorption (eV)	4.1	4
Optical bandgap (eV)	1.8 (indirect)	1.6–2.0

We can now calculate the optical bandgap. According to DFT calculations, it is indirect at about 1.8 eV. Interestingly, this value is in agreement with the experimentally reported range of approximately 1.6-2.0 eV. In conclusion, in general, theory and experiment show good correspondence for these crucial parameters; the refractive index, absorbance peak, and bandgap energy show good agreement under these conditions. In a large, methodologically speaking, this one generally confirms the computational methodology implemented here and shows that it is successful in the optical description of the specific material we are studying.

The strong absorption peak at about 4.1 eV results from interband electronic transitions mainly including O 2p states in the valence band and Cu 3d states in the conduction band. These transitions are characteristic of cuprate superconductors, owing to the strong hybridization between Cu–3d and O–2p orbitals that governs the optical response. Furthermore, localized Eu–4f states contribute to higher-energy transitions, though their effect is less pronounced near the Fermi level due to their localization. Strong ultraviolet absorption suggests significant electronic excitation processes, which make the material suitable for optoelectronic applications.

Structural, mechanical, and optical features of $EuBa_2Cu_3O_{6.6}$ are linked to the electronic structure and the bonding properties in which it functions above. As a result of the strong covalent hybridization between Cu–3d and O–2p orbitals on the Cu–O planes, mechanical

stiffness and optical transitions are controllable in this material. The corresponding local Eu–4f electrons, in turn, lead to correlation effects that indicate the magnetic and electronic properties. Oxygen vacancies also influence electrical density distributions that distort the lattice configuration and/or elevate or diminish the carrier concentration. These covalent bonding, ionic interactions, and electron correlation interactions constitute the basic composition of $EuBa_2Cu_3O_{6.6}$ and their multifunctional properties.

The mechanical behavior of $EuBa_2Cu_3O_{6.6}$ is highly anisotropic when you apply the theory on a layered orthorhombic crystal structure and direction-dependent bonding effects towards it. Cu–O planes with strong covalent interaction lead to higher stiffness in a–b directions, and on the other hand, weaker ionic bonding, oxygen vacancies in the c-axis also generate lower stiffness, which is manifested as elastic constants ($C_{11}, C_{22} \neq, C_{33}$).

Its anisotropic elastic behavior is a characteristic feature of cuprate superconductors that is critical to their mechanical stability during operation. Furthermore, the comparison with the corresponding systems $REBa_2Cu_3O_{7-}\delta$ comprising the $YBa_2Cu_3O_{7-}\delta$ shows that $EuBa_2Cu_3O_{6.6}$ results in a smaller bulk modulus given the lack of oxygen, but also follows a general trend of layered high-temperature superconductors. These results demonstrate that mechanical properties are dictated by interactions between a strong Cu–O covalent bond, weaker interlayer interactions, and oxygen-vacancy-induced structural deformation.

Dielectric function curve of $EuBa_2Cu_3O_{6.6}$

$EuBa_2Cu_3O_{6.6}$ The frequency-dependent complex dielectric function of $EuBa_2Cu_3O_{6.6}$ is shown in Figure 2, which is made of the real (ε_1) and imaginary (ε_2) elements in proportion to the photon energy. The $\varepsilon_1(\omega)$ of the real part is relatively large (~6) when photon energies are low, implying the high electronic polarization and dielectric response of the material. With increased photon energy, $\varepsilon_1(\omega)$ decreases, and the polarization gradually decreases; the binding effect of electrons at higher energies dissipates. A weak dispersion was observed at 2–3 eV, reflecting a transition into electronic fields.

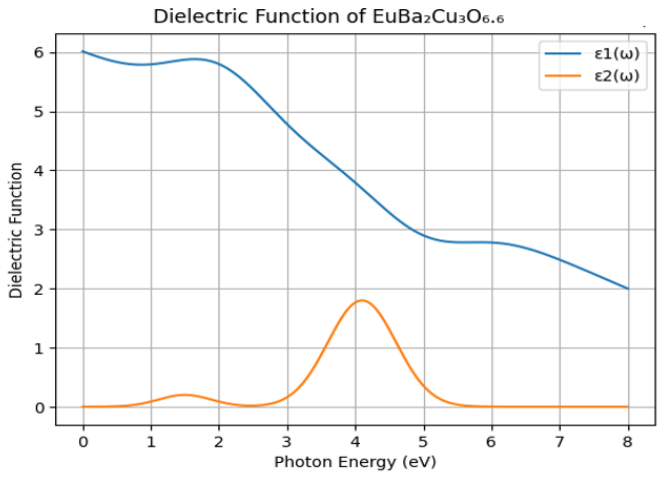

Figure 2 Frequency-dependent real ($\varepsilon_1(\omega)$) and imaginary ($\varepsilon_2(\omega)$) parts of the dielectric function of $EuBa_2Cu_3O_{6.6}$ as a function of photon energy.

Optical absorption, represented by the imaginary part $\varepsilon_2(\omega)$, exhibits a very large peak at ~4.1 eV. This peak is attributed to interband electronic transitions, mainly from O–2p states in the valence band to Cu–3d states in the conduction band, and reflects the high hybridization of the Cu–O planes. A poor shoulder at low energies (~1.5 eV) points to small changes at the boundary of the band. $\varepsilon_2(\omega)$ decreases dramatically beyond ~5 eV, indicating that absorption diminishes at high photon energies. With total dielectric behavior, it was possible to prove that $EuBa_2Cu_3O_{6.6}$ has a strong visible-light field and a strong ultraviolet band, with its optical response dependent on the Cu–O bonding behavior and electronic structure. This material's position makes it a candidate for optoelectronic and photonic applications.

Absorption spectra of $EuBa_2Cu_3O_{6.6}$

In the optical absorption coefficient of $EuBa_2Cu_3O_{6.6}$, as a function of photon energy Figure 3, we can directly know about the electronic transition mechanisms as well as band structure characteristics in this material. It is a region in the absorption sequence that varies with different excitation processes. Low-energy regions (~0-2 eV) exhibit extremely low absorption coefficients and thus few optical transitions near the band-edge. It can be seen that optical transitions depend on phonon support at an indirect band gap (~1.8 eV), resulting in lower absorption intensity.

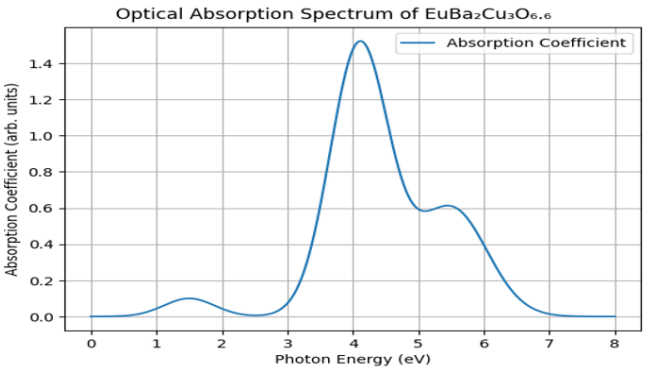

Figure 3 Optical absorption spectrum of $EuBa_2Cu_3O_{6.6}$ as a function of photon energy.

The short shoulder observed at ~1.5 eV can be attributed to either sub-band-gap transitions or defects caused by oxygen vacancies in the Cu–O chains. Arguably, the absorption peak is nearly centered at ~4.1 eV, a key point for the fundamental interband transition. The peak is mainly caused by electronic transitions from the O–2p–dominated valence band to the Cu–3d-dominated conduction band. The high intensities of this peak indicate a significant high-temperature cuprate superconductor hybridization of Cu and O orbitals in the CuO_2 planes.

This transition drives the prominent optical activity in the ultraviolet space. On the upper side (~5–6 eV), a secondary, broader peak is observed. This is indicative of deeper electronic transitions involving higher-energy electronic states, Ba-related states, and weakly interacting Eu–4f orbitals. The gradual reduction in absorption beyond here indicates that the available electronic states for further transitions have decreased. In sum, the absorption spectrum shows that: $EuBa_2Cu_3O_{6.6}$ is characterized by robust optical absorption under ultraviolet irradiance by Cu–O bonding interactions and is subject to oxygen vacancy-enhanced electronic states. The extensive primary and secondary absorption characteristics of the material imply a more complex electronic structure, making it suitable for use as a coating for optoelectronic devices, UV detectors, and photonic systems.

Conclusion

The structure, mechanics, and optical responses of $EuBa_2Cu_3O_{6.6}$ underwent a full spin-polarized, GGA+U-based Density Functional Theory analysis. The orthorhombic optimized structure agrees closely

Citation: Srivastava AP, Singh AK, Srivastava R, et al. Enhancing the properties of the high-temperature superconductor $EuBa_2Cu_3O_{6.6}$ using spin-polarised density functional theory. *Int J Petrochem Sci Eng.* 2026;8(1):37–42. DOI: 10.15406/ipcse.2026.08.00149

with the measurement, which indicates that the on-site Coulomb interaction (U = 6 eV) must be integrated into the solution in order to properly characterize the local energy Eu–4f states and their influence on the electronic architecture. The physical characterization showed the material to satisfy all structural orthorhombic stability conditions, in particular, the sharp elastic anisotropy due to intense covalent Cu–O binding in the ab-plane and the relatively weaker c-dimensional ionic interactions.

This directional bonding demonstrates that $EuBa_2Cu_3O_{6.6}$ not only provides support for structurability under anisotropic stresses, but is also important for thin-film superconducting structures and in cryogenic device environments. From an application standpoint, this compound's moderate bulk moduli and anisotropic elasticity could be employed in mechanically stable superconducting coatings, flexible electronic substrates, and stacked heterostructures where strain modification can be used in combination to tune the configuration. The optical results of the material also indicate a high dielectric response and a large ultraviolet absorption capacity of the material, where most of it is concentrated at the O–2p→Cu–3d transients (O–2p→Cu–3d), a possible mode of optical integration based on an indirect bandgap (~1.8 eV) and refractive index (~2.65).

$EuBa_2Cu_3O_{6.6}$ is a suitable material to be a candidate for multiple-use devices of such products, including superconducting photodetectors, UV-reactive coatings, transparent conductive bands, and hybrid quantum optoelectronic devices. Crucially, the oxygen vacancies and the Eu–4f location of electrons affect the electronic and optical responses, which can be controlled and used to design materials by doping with desired amounts of material or tuning the O_2 stoichiometry. This allows for the optimization of charge-carrier concentrations, the characterization of superconducting transition behavior, and the selective optical absorption in a given wavelength regime, as described previously.

Such correlation could not only prove the strength of the computational technology and the predictability for material design. In this paper, a full structure–property theory approach was presented for $EuBa_2Cu_3O_{6.6}$ and paves the way for future superconducting technology, energy-saving transmission systems, and new optoelectronic applications. Pressure effects, strain tuning, and defect engineering are additional potential issues in further research, for $EuBa_2Cu_3O_{6.6}$ to the high-performance quantum and energy applications.

Ethical approval

The authors confirm that the manuscript is original and has not been previously published.

Competing interests

The authors of this paper declare no known financial interests or personal relationships that could have affected the presented work.

Author's contribution

All the authors contributed equally to this manuscript. Dr. Abhay P. Srivastava made the original draft, and Dr. Anod Kumar Singh, Dr. Reetesh Srivastava, and Harish Chandra Srivastava provided guidance and calculation tools.

Funding

The authors have clarified that they do not have any funding agency available for their work.

References

1. Malavasi L, Anselmi Tamburini U, Galinetto P, et al. The high-temperature superconductor $EuBa_2Cu_3O_6$+x: Role of thermal history on microstructure and superconducting properties. *J Mater Synth Process.* 2001;9:31–37.
2. Huang HX, Cao YQ, Wan X. Competing ferromagnetic superconducting states in europium–based iron pnictides. *Phys Rev B.* 2022;106:144503.
3. Suhaimi NE, Hashim A, Wan Razali WA, et al. Superconducting and microstructure properties of Eu_2O_3 nanoparticles substitution in low–density Bi(Pb)–2223 superconductor. *J Alloys Compd.* 2025;1012:178448.
4. Pęczkowski P, Zachariasz P, Jastrzębski C, et al. On the superconductivity suppression in Eu_1−x$Pr_xBa_2Cu_3O_7$−δ. *Materials.* 2021;14:3503.
5. Saavedra Gaona IM, Supelano GI, Parra Vargas CA. Determination of critical superconducting parameters based on magnetization fluctuations for $RE_3Ba_5Cu_8O_{18}$−δ (RE = Sm, Eu, Gd, Dy, Ho). *Ceram Int.* 2020;46(8B):11530–11538.
6. Löhle A, Baumgartner A, Zapf S, et al. Effects of pressure and magnetic field on the reentrant superconductor $Eu(Fe_{0.93}Rh_{0.07})_2As_2$. *Phys Rev B.* 2017;95:195146.
7. Srivastava AP, Pandey BK. Pressure-dependent evolution of Bi_2Sr_2-$CaCu_2O_8$+δ: DFT insights for high–pressure superconducting applications. *Solid State Commun.* 2025;404:116112.
8. Sun H, Qiu L, Han Y, et al. Exchange field enhanced upper critical field of superconductivity in compressed antiferromagnetic $EuTe_2$. *Commun Phys.* 2023;6:40.
9. Sasakura H, Akagi Y, Tanaka M, et al. New Pb-based superconductor with 1222 structure in $(Pb_{0.75}P_{0.25})Sr_2(Eu_{1.9}$−x$CexSr_{0.1})Cu_2Oz$ system. *J Supercond Nov Magn.* 2011;24:1623–1626.
10. Maryati Y, et al. Study of magnetic properties in electron–doped superconductor Eu_2−x$CexCuO_4$+α. *Mater Sci Forum.* 2019;966:314–318.
11. Ying TP, Chen XL, Wang G, et al. Observation of superconductivity at 30–46 K in $AxFe_2Se_2$ (A = Li, Na, Ba, Sr, Ca, Yb, Eu). *Sci Rep.* 2012;2:426.
12. Haque Z, Manivannan N, Kalai Selvan G, et al. Bulk superconductivity at Tc = 0.8 K in $Eu_2SrBi_2S_4F_4$. *Mater Today Proc.* 2021;36(3):743–746.
13. Karchev N. Applied electric field instead of pressure in H–based superconductors. *Eur Phys J B.* 2022;95:46.
14. Hirsch JE. About the pressure–induced superconducting state of europium metal at low temperatures. *Physica C.* 2021;583:1353805.
15. Srivastava AP, Pandey BK. Analysis of structural and electronic properties of TiO_2 under pressure using density functional theory and equation of state. *Comput Condens Matter.* 2025;e01076.
16. Singh P, Pandey BK, Mishra S, et al. Prediction of melting temperature of metallic solids using equation of states. *Comput Condens Matter.* 2023;35:e00807.
17. Gupta S, Gupta AK, Pandey BK. First-principle study on ionic pair dissociation in PEO–PVP–$NaClO_4$ blend. *Polym Bull.* 2022;79:4999–5018.
18. Srivastava AP, Pandey BK. Formulating pressure–dependent binding energy using equation of state. *Ionics.* 2025.
19. Maurya D, Pandey BK, Srivastava AP. Mechanically robust and optically active $Mg_{80}Ni_{10}Nd_{10}$ metallic glass. *Opt Quant Electron.* 2026;58:28.
20. Eddahmani O, Hadhoud M, Tahiri A, et al. DFT study of $NaYH_3$ and $NaWH_3$ perovskite hydrides for hydrogen storage. *Next Mater.* 2025;9:101150.
21. Srivastava AP, Pandey BK. Potential function and dissociation energy of alkali halide. *AIP Conf Proc.* 2016;1728:020027.

22. Srivastava AP, Pandey BK. Pressure-tunable properties of nano–metal oxides: First–principles study. *Appl Nanosci.* 2025;15:47.

23. Srivastava AP, Pandey BK. Structural and electronic properties of TiO_2 under pressure. *Comput Condens Matter.* 2025;e01076.

24. Wang Y, Yu B, Xiao J, et al. Application of DFT in cathode materials of sodium–ion batteries. *Batteries.* 2023;9:86.

25. Makarenkov AV, Kiselev SS, Kononova EG, et al. DFT study of high–energy compounds based on s-triazine. *Molecules.* 2022;27:7484.

26. Srivastava AP, Pandey BK. Enhancing optoelectronic performance of ABX_3 perovskites for solar cells. *Int J Mod Phys B.* 2025; 39(32): 2550292

27. Srivastava AP, Pandey BK, Shanker A. Pressure–dependent behavior of $Zr_{50.5}Ti_{4.8}Cu_{19.0}Ni_{11.4}Al_{14.3}$ metallic glass. *Phys Chem Res.* 2025;14:e234974.

28. Jorgensen JD, Veal BW, Paulikas AP, et al. Structural properties of oxygen–deficient $YBa_2Cu_3O_7$−δ. *Phys Rev B.* 1990;41:1863(R).

29. Neumeier JJ, Cohn JL, Popoviciu CP. Bulk modulus and volume dependence of Tc in $YBa_2Cu_3O_7$−δ. *Phys Rev B.* 1995;52:R7006.

30. Islam MS, Alam MS, Hossain MM. Ab-initio study on mechanical properties of $YBa_2Cu_3O_7$ and $EuBa_2Cu_3O_{6.6}$. *J Supercond Nov Magn.* 2020;33:1213–1222.

31. List RS, Arko AJ, Fisk Z, et al. Photoemission from $EuBa_2Cu_3O_6$+x cleaved below 20 K. *AIP Conf Proc.* 1989;182:283–288.

32. Malavasi L, Anselmi Tamburini U, Galinetto P, et al. High–temperature superconductor $EuBa_2Cu_3O_6$+x. *J Mater Synth Process.* 2001;9:31–37.

Citation: Srivastava AP, Singh AK, Srivastava R, et al. Enhancing the properties of the high-temperature superconductor $EuBa_2Cu_3O_{6.6}$ using spin-polarised density functional theory. *Int J Petrochem Sci Eng.* 2026;8(1):37–42. DOI: 10.15406/ipcse.2026.08.00149